

PARTIAL WAVE ANALYSIS OF $J/\psi \rightarrow \gamma\eta\pi^+\pi^-$ *

T. Bolton,^(e) J. S. Brown,^(f) K. O. Bunnell,^(e) M. Burchell,^(b) T. H. Burnett,^(f)
R. E. Cassell,^(e) D. Coffman,^(a) D. H. Coward,^(e) P. Coyle,^(b) F. DeJongh,^(a)
J. Drinkard,^(b) G. P. Dubois,^(a) G. Eigen,^(a) B. I. Eisenstein,^(c) T. Freese,^(c)
C. Gatto,^(b) G. Gladding,^(c) C. A. Heusch,^(b) D. G. Hitlin,^(a) J. M. Izen,^(c)
P. C. Kim,^(e) J. Labs,^(e) A. Li,^(f) W. S. Lockman,^(b) U. Mallik,^(d)
C. G. Matthews,^(a) R. Mir,^(f) P. M. Mockett,^(f) A. Odian,^(e) L. Parrish,^(f)
D. Pitman,^(e) J. D. Richman,^(a) H. F. W. Sadrozinski,^(b) M. Scarlatella,^(b)
T. L. Schalk,^(b) R. H. Schindler,^(e) A. Seiden,^(b) I. E. Stockdale,^(c)
W. Toki,^(e) B. Tripsas,^(c) M. Z. Wang,^(d) A. J. Weinstein,^(b) S. Weseler,^(b)
H. J. Willutzki,^(f) W. J. Wisniewski,^(a) R. Xu,^(b) and Y. Zhu^(a)

The Mark III Collaboration

- (a) *Department of Physics, California Institute of Technology, Pasadena, CA 91125.*
- (b) *Santa Cruz Institute for Particle Physics, University of California, Santa Cruz, CA 95064.*
- (c) *Department of Physics, University of Illinois at Urbana-Champaign, Urbana, IL 61801.*
- (d) *Department of Physics, University of Iowa, Iowa City, IA 52242.*
- (e) *Stanford Linear Accelerator Center, Stanford University, Stanford, CA 94309.*
- (f) *Department of Physics, University of Washington, Seattle, WA 98195.*

Submitted to *Physical Review Letters*.

* Work supported in part by the Department of Energy contracts DE-AC03-76SF00515, DE-AC02-76ER01195, DE-AC02-76ER03130, DE-AC03-81ER40050, DE-AM03-76SF00010, and by the National Science Foundation.

Abstract

We present a study of the decay $J/\psi \rightarrow \gamma\eta\pi^+\pi^-$ using the Mark III detector at SPEAR. A partial wave amplitude analysis is performed on the $\eta\pi^+\pi^-$ system in the mass region from 1.2 to 1.5 GeV. We observe two $\eta\pi^+\pi^-$ resonances, each decaying via $a_0(980)\pi$. We identify one as the axial vector meson $f_1(1285)$ and the other as a pseudoscalar resonance at 1.40 GeV.

PACS Numbers 13.25, 14.40

Since it was first observed in radiative J/ψ decays by the Mark II¹ and Crystal Ball² collaborations, much effort has been devoted to the study of the $\eta(1440)$ (formerly the $\iota(1440)$). This state has been considered by many³ to be a prime candidate for gluonium (a bound state of two gluons), since it is copiously produced in radiative J/ψ decays⁴ and is not observed in $\gamma\gamma$ collisions.⁵ In addition, the spin-parity assignment of $J^{PC} = 0^{-+}$ made it difficult to classify the $\eta(1440)$ into the lowest-lying quark-antiquark nonets.⁶

Results from an early amplitude analysis² indicated that the $\eta(1440)$ decays through the $J^{PC} = 0^{-+}$ $a_0(980)\pi$ (S-wave) intermediate state into $K\bar{K}\pi$, where $a_0(980) \rightarrow K\bar{K}$. Since $\eta\pi$ is the other dominant decay mode of the $a_0(980)$, the $\eta(1440)$ was searched for in the decay $J/\psi \rightarrow \gamma\eta\pi^+\pi^-$. No signal resembling the broad $K\bar{K}\pi$ enhancement was seen at 1.44 GeV in the $\eta\pi^+\pi^-$ invariant mass distribution. Instead, a narrower signal near 1.39 GeV was observed.⁷

In order to perform a more sensitive search for states in the 1.2 to 1.5 GeV mass region, the decays $J/\psi \rightarrow \gamma K\bar{K}\pi$ and $J/\psi \rightarrow \gamma\eta\pi^+\pi^-$ have been studied by the Mark III collaboration, using an isobar model partial wave amplitude (PWA) analysis method.⁸ The results of the $K\bar{K}\pi$ study⁹ indicate that the $\eta(1440)$ is not adequately described as a single resonance, but rather as a superposition of several states. These include a pseudoscalar state near 1.41 GeV decaying through $a_0(980)\pi$, an axial vector state near 1.44 GeV decaying through K^*K , and a second pseudoscalar state near 1.49 GeV decaying through K^*K . We report herein the results of a PWA analysis of the decay $J/\psi \rightarrow \gamma\eta\pi^+\pi^-$ and compare the parameters of the states found in this analysis with those obtained in the $K\bar{K}\pi$ channel and in hadron-induced reactions.

This analysis is based upon a sample of 5.8×10^6 produced J/ψ events collected with the Mark III detector¹⁰ at the SLAC e^+e^- storage ring SPEAR. The data

presented here contain only photons and charged pions in the final state. The photons are detected in an electromagnetic calorimeter (a barrel and two endcaps) with total coverage 94% of 4π . The charged tracks are detected in a multilayer cylindrical drift chamber which covers 85% of 4π .

In our analysis the η is detected in its $\gamma\gamma$ and $\pi^+\pi^-\pi^0$ decays. We select events with no net charge and the required number of charged tracks ($n_{ch} = 2$ for $\eta \rightarrow \gamma\gamma$ and $n_{ch} = 4$ for $\eta \rightarrow \pi^+\pi^-\pi^0$) and showers ($n_{sh} \geq 3$).¹¹ We require that the energy of each shower be greater than 100 MeV for $n_{ch} = 2$, and greater than 50 MeV for $n_{ch} = 4$. Four-constraint (4C) kinematic fits are performed to the hypotheses $J/\psi \rightarrow \gamma\gamma\pi^+\pi^-$ and $J/\psi \rightarrow \gamma\gamma\pi^+\pi^-\pi^+\pi^-$. If $n_{sh} > 3$, the fit is repeated using all possible combinations of three candidate photons. For events with a good fit, the combination with the largest probability of χ^2 ($P(\chi^2)$) is selected. For $n_{ch} = 2$, events with a 5C fit are retained if $P(\chi^2) > 10\%$ (the extra constraint is that of the η mass). For $n_{ch} = 4$, a 6C fit with $P(\chi^2) > 10\%$ is required (π^0 and η mass constraints are imposed). Backgrounds are suppressed by removing asymmetric decays of the π^0 and η . The selected data sample contains feedthrough from other decays (e.g. $J/\psi \rightarrow \rho\pi$ and $\omega\pi$ for $n_{ch} = 2$ and $J/\psi \rightarrow \pi^+\pi^-\pi^+\pi^-\pi^0$ for $n_{ch} = 4$). This is compatible with known rates plus Monte Carlo (MC) studies. We find that we can efficiently remove these contaminations by rejecting events satisfying 4C fits to $J/\psi \rightarrow \gamma\gamma\pi^+\pi^-$, $\gamma\gamma\gamma\pi^+\pi^-$ or a 5C fit to $J/\psi \rightarrow \pi^+\pi^-\pi^+\pi^-\pi^0$. This rejection does not bias the selection of the genuine signal.

The $\eta\pi^+\pi^-$ mass distributions from the decay $J/\psi \rightarrow \gamma\eta\pi^+\pi^-$ are shown in Figure 1 for both decay modes of the η . The dominant feature is the η' signal (inset), and both channels show significant structures at higher masses. Slight differences between the spectra in the two final states are apparent, reflecting differences in

statistics, backgrounds, and above 2.8 GeV the effect of the differing photon energy criteria.

To check that the data selection and reconstruction methods are well understood, we measure the branching ratio $B(J/\psi \rightarrow \gamma\eta')$. Signal strengths in both final states are found by fitting the invariant mass distributions with a non-relativistic Breit–Wigner function convoluted with a gaussian mass resolution term (henceforth abbreviated as BWG). The mass resolution ($\sigma = 0.009$ GeV) and the efficiency for finding a signal in an analysis are found by MC simulation.¹² We find:

$$B(J/\psi \rightarrow \gamma\eta') = (4.50 \pm 0.14 \pm 0.53) \times 10^{-3}$$

and

$$B(J/\psi \rightarrow \gamma\eta') = (4.30 \pm 0.31 \pm 0.71) \times 10^{-3} \quad ,$$

for the $\eta \rightarrow \gamma\gamma$ and $\eta \rightarrow \pi^+\pi^-\pi^0$ mode, respectively. The first error given is statistical, the second systematic. The systematic errors include several terms added in quadrature. These reflect the uncertainties in the J/ψ flux (8.5%), the MC simulation (6.5% for $n_{ch} = 2$, 7.1% for $n_{ch} = 4$), the fit of the BWG function to the data (0.5% for $n_{ch} = 2$, 3.7% for $n_{ch} = 4$), and the effect of varying the selection criteria (5.1% for $n_{ch} = 2$, 11.9% for $n_{ch} = 4$). The results are compatible with previous measurements.^{13,14}

In the PWA analysis the amplitudes are constructed from Lorentz invariant combinations of the momenta and polarization 4-vectors¹⁵ in the events. We consider the process as a three-step sequential decay $J/\psi \rightarrow \gamma X, X \rightarrow AP, A \rightarrow PP$, where X and A are intermediate resonances, and the P 's are pseudoscalars (π or η). The relative magnitudes and phases of the amplitudes are found by a maximum likeli-

hood (\mathcal{L}) fit to the data. The bin-to-bin variation in magnitude and phase of each amplitude reveals the presence of any resonance(s) X .

We consider $J^{PC}(X) = 0^{-+}$ or 1^{++} , and allow X to decay to $a_0(980)\pi$ or $f_0(1400)\eta$. The $a_0(980)$ is included on the basis of studies of $\eta\pi^\pm$ invariant masses in our data. To parametrize the $a_0(980)$ line shape we use a relativistic coupled-channel propagator.¹⁶ We include $f_0(1400)$ on the grounds that, due to its large width, it cannot be excluded *a priori*. The $f_0(1400)$ propagator is parametrized using the formalism of an S-wave $\pi\pi$ scattering amplitude with a pole at 1.4 GeV.¹⁷ To account for events not described by the above amplitudes, we include an additional amplitude which is not allowed to interfere with the others, and corresponds to a phase space decay of X . We fit the data in 0.02 GeV $\eta\pi^+\pi^-$ mass bins. Monte Carlo studies indicate that the $\eta\pi^+\pi^-$ mass resolution (σ) increases from 0.011 to 0.013 GeV in the 1.2 to 1.5 GeV mass range.

To test the ability of the PWA analysis to identify amplitudes correctly, we generate MC signals of various J^{PC} values with statistics similar to that of the data. After analysis we find that the MC signals are correctly identified. The goodness of each fit is checked by comparing the fit predictions of various two-body invariant mass and angular distributions with those occurring in the generated data. Good agreement is found.

Analyzing the data in Figure 1 up to $\eta\pi^+\pi^-$ masses of 1.6 GeV, the quantity $\ln \mathcal{L}$ divided by the number of events in each mass bin varies from 0.25 to 0.4. Similar results are obtained in MC studies. The two-body invariant mass and angular distributions are also well reproduced. Above 1.6 GeV the model no longer reproduces these distributions and the goodness of fit decreases. Hence we restrict our analysis to the 1.2 to 1.5 GeV mass region.

We find that the $1^{++}f_0(1400)\eta$ amplitude contributes negligibly and is thus excluded in subsequent analysis. The $0^{-+}f_0(1400)\eta$ amplitude has a nonzero magnitude in the higher statistics $\eta \rightarrow \gamma\gamma$ sample, but shows no evidence for a $\eta\pi^+\pi^-$ resonance, nor does it improve the likelihood of the fit significantly.¹⁸ Accordingly, we repeat the analysis with no $0^{-+}f_0(1400)\eta$ contribution. The previous $0^{-+}f_0(1400)\eta$ events now appear in the phase space term, and the contributions to the other amplitudes remain unchanged. These results (i.e., using only the set of $a_0(980)\pi$ amplitudes plus phase space term) are shown in Figure 2, and the relative phases in Figure 3, together with the corresponding data from the $\eta \rightarrow \pi^+\pi^-\pi^0$ sample.

In the $\eta \rightarrow \gamma\gamma$ final state, we observe two clear features: a resonant structure in $1^{++}a_0(980)\pi$ at ~ 1.3 GeV, and in $0^{-+}a_0(980)\pi$ at 1.4 GeV. This is borne out both in the magnitude of the amplitudes and in the phase motion. A single fit to the whole of the $1^{++}a_0(980)\pi$ spectrum in Figure 2(a) fails. We therefore extract the component of the spectrum compatible with the well-known resonance $f_1(1285)$. The $f_1(1285)$ line shape (modelled by a BWG function with mass, width and mass resolution parameters of 1.282,¹³ 0.024¹³ and 0.011 GeV, respectively) is shown as a solid curve in Figure 2(a). The area below the solid curve is normalized to that of the data in the mass range 1.24 to 1.32 GeV. In this mass range we find the ratio of the magnitude of the helicity 1 to helicity 0 amplitudes to be 0.64 ± 0.07 . Above 1.32 GeV, there is an excess in $1^{++}a_0(980)\pi$ beyond that expected for $f_1(1285)$. This remains independent of the inclusion or exclusion of the $f_0(1400)\eta$ amplitudes in the PWA analysis, or when the event selection criteria are varied. To better understand this region a much larger data set is needed. We consider the structure in the 1.34 to 1.36 GeV bin in Figure 2(a) a fluctuation since it appears to be narrower than our mass resolution. In addition we note that we see no associated phase motion in this bin nor a similar structure in the $\eta \rightarrow \pi^+\pi^-\pi^0$ sample.

In the $0^{-+}a_0(980)\pi$ amplitude we see a clear resonant structure (henceforth referred to as $\eta(1400)$). We fit it with a BWG function ($\sigma = 0.013$ GeV), obtaining a mass of (1.400 ± 0.006) GeV, and a width Γ of (0.047 ± 0.013) GeV. The fitted line shape is shown solid curve in Figure 2(b).

Having determined the efficiency from MC simulation and studies of the η' signal we find the branching ratios for these two signals:

$$\begin{aligned} & \text{B}(J/\psi \rightarrow \gamma f_1(1285)) \text{B}(f_1(1285) \rightarrow a_0(980)\pi) \text{B}(a_0(980) \rightarrow \eta\pi) \\ & = (2.60 \pm 0.28 \pm 0.58) \times 10^{-4} \end{aligned}$$

$$\begin{aligned} & \text{B}(J/\psi \rightarrow \gamma \eta(1400)) \text{B}(\eta(1400) \rightarrow a_0(980)\pi) \text{B}(a_0(980) \rightarrow \eta\pi) \\ & = (3.38 \pm 0.33 \pm 0.64) \times 10^{-4} \end{aligned}$$

The systematic error is determined in a manner similar to that for $\text{B}(J/\psi \rightarrow \gamma\eta')$, with the addition of the following extra terms. To reflect the accuracy of the PWA analysis we add the spread in the results of the PWA analysis of a set of MC generated signals with statistics similar to the real data (15.5%). The change in the efficiency (2%) for various combinations of 1^{++} helicity ratios is included for the $f_1(1285)$ branching fraction. We include a term reflecting the uncertainty in the magnitude of the non-resonant background [11% for $f_1(1285)$ and 7.7% for $\eta(1400)$].

The $\eta \rightarrow 3\pi$ final state shows features compatible with those seen in the $\eta \rightarrow \gamma\gamma$ channel. The line shapes in Figs. 2(d) and 2(e) use the same masses, widths and normalizations (including relative η branching fractions) as those in Figs. 2(a) and 2(b), respectively. The agreement of the estimated signal strengths with the data illustrates the high degree of compatibility of the two final state samples. The lower statistics and uncertainties in the low energy γ reconstruction efficiency prevent

precise branching fraction determinations in the $\eta \rightarrow 3\pi$ channel. However, due to the more highly constrained η selection this channel has less background [cf. Figs. 2(c) and 2(f)], indicating that the $\eta\pi^+\pi^-$ data in this mass range are dominated by $a_0(980)\pi$ amplitudes.

In conclusion, we present a PWA analysis of the decay $J/\psi \rightarrow \gamma\eta\pi^+\pi^-$ in two independent η decay channels, over the 1.2 to 1.5 GeV $\eta\pi^+\pi^-$ mass range. In each channel we observe two signals, both decaying via $a_0(980)\pi$. We identify the 1^{++} signal at mass 1.29 GeV with the well-known axial vector state $f_1(1285)$. The results show an excess of data at masses slightly above that of the $f_1(1285)$; an improvement in statistics is needed to investigate it definitively. The signal at mass (1.400 ± 0.006) GeV has a width Γ of (0.047 ± 0.013) GeV and $J^{PC} = 0^{-+}$. We identify the $\eta(1400)$ with a similar signal seen in an analogous PWA analysis of the $K\bar{K}\pi$ system in $J/\psi \rightarrow \gamma K\bar{K}\pi$.⁹ That analysis observes a 0^{-+} signal at 1.416 GeV with a width of 0.054 GeV, decaying via $a_0(980)\pi$, the low mass component of the “iota” (this is also seen elsewhere¹⁹). There is evidence for a similar $\eta(1400)$ state in other reactions. In the charge exchange reaction $\pi^-p \rightarrow \eta\pi^+\pi^-n$, a 0^{-+} signal has been observed around 1.4 GeV, again decaying via $a_0(980)\pi$.^{20,21} We note, however, that central production, $pp \rightarrow p(\eta\pi\pi)p$ at 300 GeV incident p momentum,²² yields no resonant signal around 1.4 GeV, just as the analogous process $p\bar{p} \rightarrow p(K\bar{K}\pi)p$ fails to find a 1.4 GeV signal decaying to $K\bar{K}\pi$ via $a_0(980)\pi$.²³

We can combine our observation of the $f_1(1285)$ (a well-known axial vector meson) with our measurement in the similar channel $J/\psi \rightarrow \gamma\pi^+\pi^-\pi^+\pi^-$,²⁴ to obtain a total rate for its production in radiative J/ψ decays (a two-gluon-mediated process) which is compatible with predictions from perturbative QCD calculations incorporating longitudinal gluons.²⁵ Whether the $\eta(1400)$ is a $q\bar{q}$ state or a gluonic meson is not determined.

We acknowledge the support of SLAC's SPEAR and linear accelerator operating staff. G. Eigen acknowledges the support of the Heisenberg Foundation. This work was supported in part by Department of Energy contracts DE-AC03-76SF00515, DE-AC02-76ER01195, DE-AC02-76ER03130, DE-AC03-81ER40050, DE-AM03-76SF00010, and by the National Science Foundation.

References

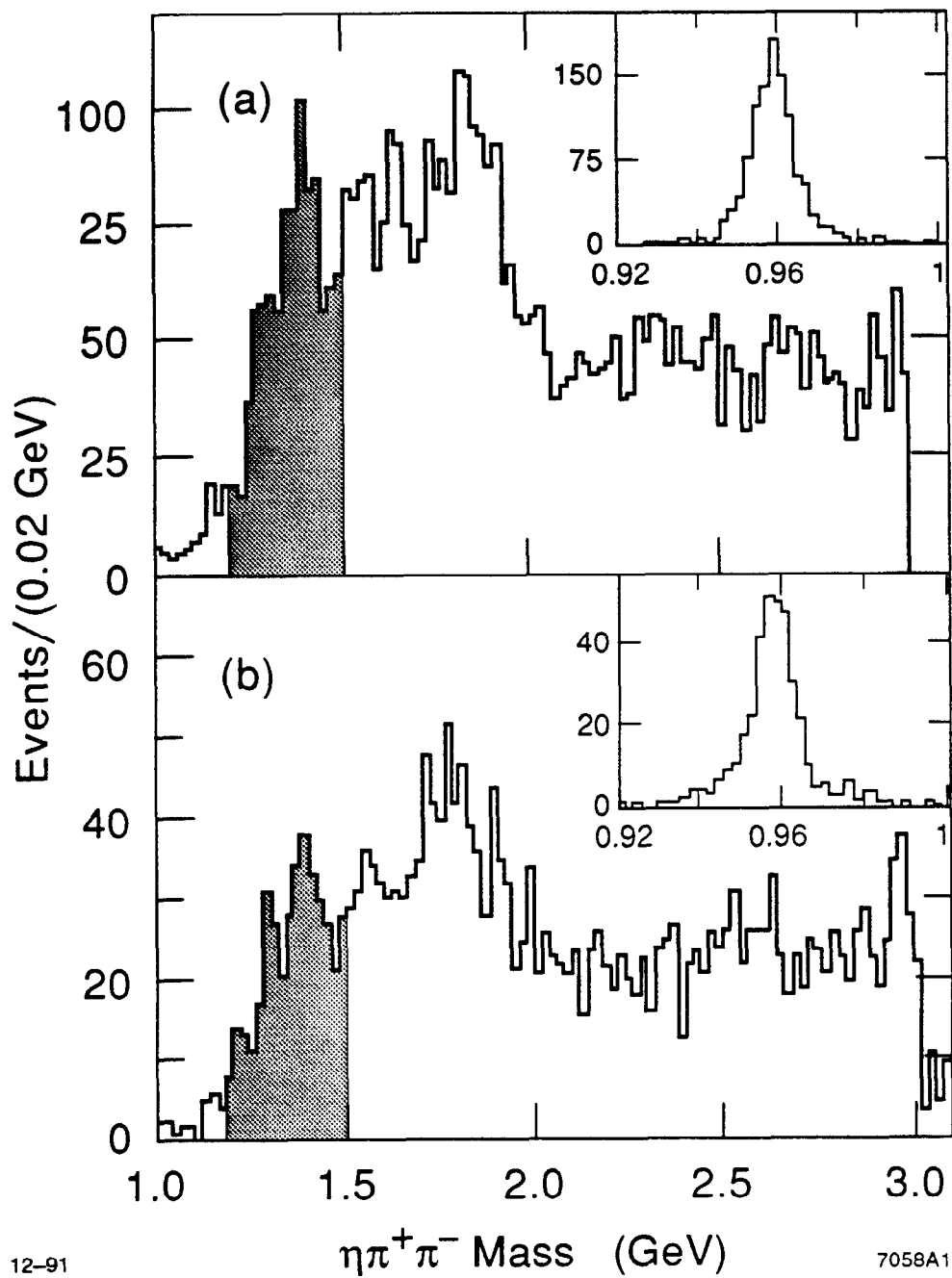
1. D. Scharre *et al.*, Phys. Lett. **97B**, 329 (1980).
2. C. Edwards *et al.*, Phys. Rev. Lett. **49**, 259 (1982).
3. See, for example: M. Chanowitz, Nucl. Phys. **A527**, 61 (1991).
4. To lowest order in perturbative Quantum Chromodynamics, the amplitude for the decay $J/\psi \rightarrow \gamma + X$ proceeds through the exchange of two gluons in an SU(3) color and flavor singlet. These gluons may resonate to form gluonic mesons.
5. The most stringent upper limit for the $\eta(1440)$ $\gamma\gamma$ width ($\Gamma(\gamma\gamma)$) times its $K\bar{K}\pi$ branching ratio ($B(K\bar{K}\pi)$) is $\Gamma(\gamma\gamma) \times B(K\bar{K}\pi) < 1.7$ keV. See: H. Behrend *et al.*, , Z. Phys. **C42**, 367 (1989).
6. The ground state pseudoscalar nonet is already filled. Candidates for the $I = 0$ members of the first radially excited pseudoscalar nonet include the established $\eta(1295)$ state (Reference 13) and the $\eta(1400)$ (See References 9, 20 and 21.)
7. J. Becker *et al.*, contributed paper to the 23rd Int. Conf. on High Energy Physics, Berkeley, July, 1986 and SLAC-PUB-4246 (1987) (unpublished).
8. D. Herndon, P. Söding and R. J. Cashmore, Phys. Rev. **D11**, 3165 (1984).
9. Z. Bai *et al.*, Phys. Rev. Lett. **65**, 2507 (1990).
10. D. Bernstein *et al.*, Nucl. Instr. & Meth. **226**, 301 (1983).
11. Showers (clusters of energy in the electromagnetic shower counter not associated with charged tracks) must be in the well-modeled regions of the detector, away from the barrel-endcap transition regions and barrel supports. Hadronic interactions are not fully recognized and suppressed in the analysis, so events can contain extra (non photon) showers.

12. The MC simulates the full detector performance and includes the predicted angular distribution for any decay.
13. Review of Particle Properties, Phys. Rev. **D45 S1**, 1 (1992).
14. J. E. Augustin *et al.*, Phys. Rev. **D42**, 10 (1990).
15. C. Zemach, Phys. Rev. **133**, B1201 (1964).
16. For the $a_0(980)$, we assume a pole mass, width and coupling constant ratio $(g_{KK}/g_{\eta\pi})^2$ of 0.983 GeV, 0.082 GeV, and 1.5, respectively. The final results are not sensitive to small variations in these parameters. Details of the $a_0(980)$ parametrization are given in: N. A. Tornqvist, Ann. Phys. **123**, 1 (1979); N. N. Achasov, S. A. Devyanin and G. N. Shestakov, Sov. J. Nucl. Phys. **32**, 566 (1980).
17. P. Estabrooks and A. Martin, Nucl. Phys. **B95**, 322 (1975). The $f_0(1400)$ is also parametrized using a standard relativistic S-wave Breit–Wigner propagator whose width was varied from 0.1 to 0.4 GeV. No significant changes in the final results are observed due to these different $f_0(1400)$ parametrizations.
18. The presence of this amplitude can cause interference in the intensity distributions, reducing the width of the signal seen in the $0^{-+} a_0(980)\pi$ amplitude at 1.40 GeV. This is due to low statistics and acceptance in certain fiducial regions.
19. A. Birman *et al.*, Phys. Rev. Lett. **61**, 1557 (1989); M. G. Rath *et al.*, Phys. Rev. **D40**, 693 (1989).
20. A. Ando *et al.*, Phys. Rev. Lett. **57**, 1296 (1986).
21. S. Fukui *et al.*, Phys. Lett. **B267**, 293 (1991).
22. T. A. Armstrong *et al.*, Z. Phys. **C52**, 389 (1991).

23. T. A. Armstrong *et al.*, Phys. Lett. **146B**, 273 (1984); Z. Phys. **C34**, 23 (1987);
Phys. Lett. **221B**, 216 (1989).
24. T. Bolton *et al.*, , Phys. Lett. **B278**, 495 (1992).
25. J. Körner *et al.*, Nucl. Phys. **B229**, 115 (1983).

Figure Captions

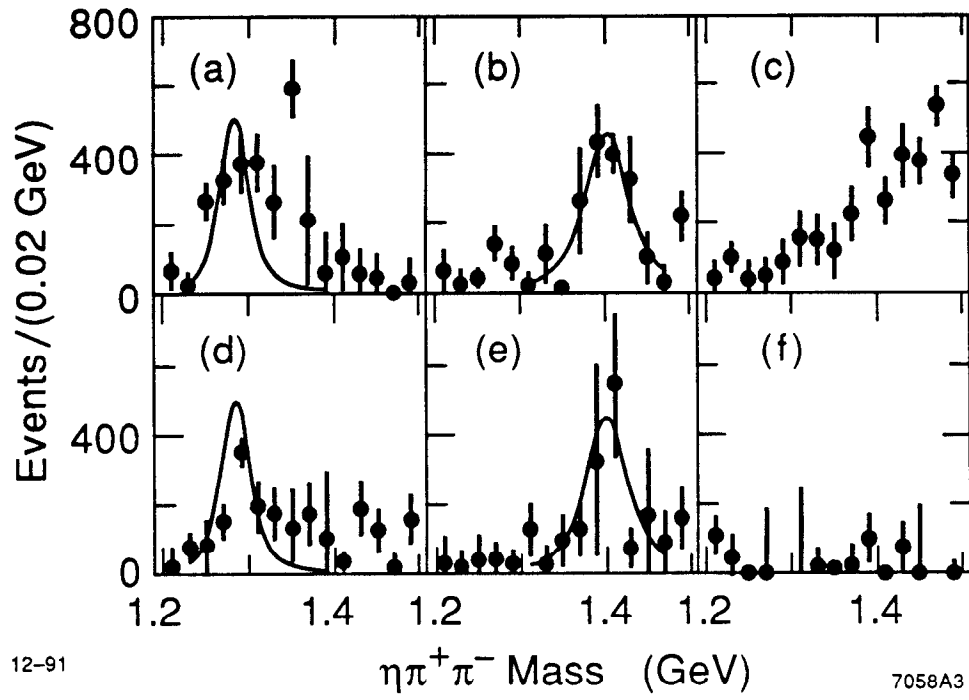
1. The $\eta\pi^+\pi^-$ invariant mass distribution above 1 GeV for the (a) $\eta \rightarrow \gamma\gamma$, and (b) $\eta \rightarrow \pi^+\pi^-\pi^0$ channels. The shaded region is that subjected to the PWA analysis. In both channels, the mass distribution below 1 GeV is shown in an inset with 0.002 GeV bin width.
2. Acceptance corrected intensity distributions using the channel $\eta \rightarrow \gamma\gamma$: (a) $1^{++} a_0(980)\pi$; (b) $0^{-+} a_0(980)\pi$; (c) phase space; (d), (e) and (f) are, respectively, the same for the $\eta \rightarrow \pi^+\pi^-\pi^0$ channel.
3. Phase difference between $a_0(980)\pi$ amplitudes using ($\eta \rightarrow \gamma\gamma$ channel): (a) 1^{++} relative to 0^{-+} ; (b) 0^{-+} relative to 1^{++} ; (c) and (d) are, respectively, the same for the $\eta \rightarrow \pi^+\pi^-\pi^0$ channel. An arbitrary zero point is used for each figure.



12-91

7058A1

Fig. 1



12-91

7058A3

Fig. 2

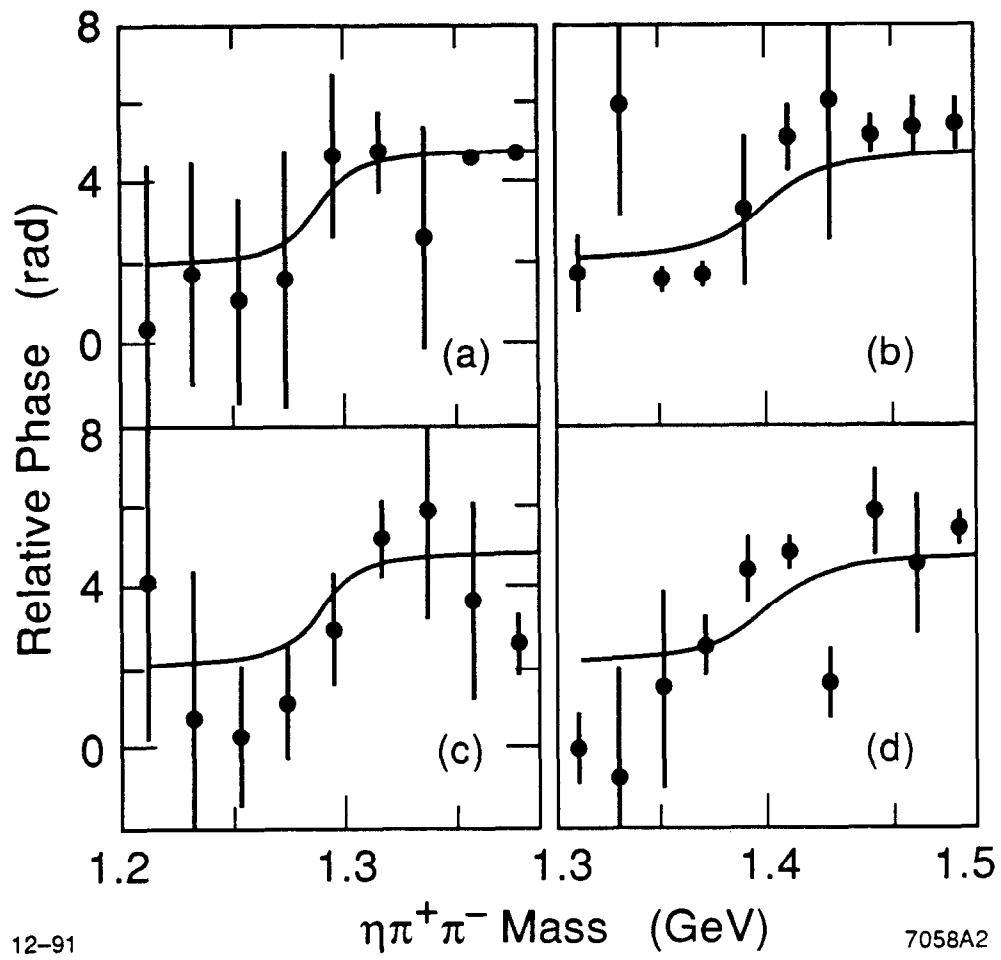


Fig. 3